SLAC–95–6787
June 1995

A BUNCH COMPRESSOR FOR THE NEXT LINEAR COLLIDER *

P. Emma, T. Raubenheimer, F. Zimmermann,
Stanford Linear Accelerator Center, Stanford University, Stanford CA 94025 USA

Abstract

A bunch compressor design for the Next Linear Collider (NLC) is described. The compressor reduces the bunch length by a factor of 40 in two stages. The first stage at 2 GeV consists of an rf section and a wiggler. The second stage at 10 GeV is formed by an arc, an rf section, and a chicane. The final bunch phase is insensitive to initial phase errors and to beam loading in the intermediate S-band pre-linac. Residual longitudinal aberrations of the system are partially compensated. The bunch compressor encompasses a solenoid spin-rotator system at 2 GeV that allows complete control over the spin orientation.

I. INTRODUCTION

The purpose of the NLC bunch compressor is to reduce the bunch length, which is about 4 mm at extraction from the damping rings, to 100 μm, suitable for injection into the main X-band linac. The bunch compressor may have to compensate bunch-to-bunch phase errors due to beam-loading in the damping ring unless the latter is compensated by some other means. This requires a rotation by $\pi/2$ in the longitudinal phase space so that phase errors are converted into energy errors. The compressor also has to compensate for beam-loading effects originating in its various accelerating sections, and it provides a trombone-like arm, reversing the direction of the beam before injection into the main linac. This gives space for abort systems, allows feed-forward from the ring to the linac, and facilitates future upgrades. Furthermore, the bunch compressor includes a spin-rotator system, and provides tuning elements and diagnostics to correct dispersion and coupling. To determine the optimum parameters of the system, three different scenarios are considered, denoted NLC I, NLC II and NLC III, corresponding to different upgrade stages (see Table I).[1]

Table 1. Three different NLC scenarios.

	NLC I	NLC II	NLC III
c.m. energy	500 GeV	1 TeV	1.5 TeV
gradient	36.7 MV/m	61 MV/m	75 MV/m
main linac length	6.9 km	8.3 km	10 km
N/bunch	$0.66 \cdot 10^{10}$	$1.1 \cdot 10^{10}$	$1.5 \cdot 10^{10}$

The proposed bunch compressor comprises two stages and an intermediate S-band pre-linac that accelerates the beam from 2 GeV to 10 GeV [2]. The design is illustrated in Figure 1.

*Work supported by Department of Energy contract DE-AC03-76SF00515

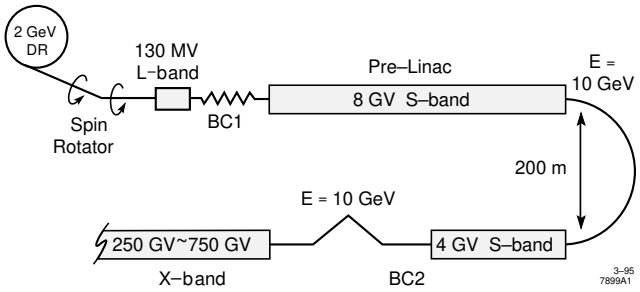

Figure. 1. Schematic of the NLC bunch compressor.

The parameters of the compressor system are chosen such that, first, the energy spread at the end of the X-band linac is smaller than the bandwidth of the final focus system; second, no significant energy tails are generated; and third, both the mean energy and the energy spread at the end of the linac are insensitive to phase and energy errors resulting from beam loading in damping rings and pre-linac, respectively. The phase error at extraction from the damping ring may be as large as 20° S-band (or 6 mm), while at the end of the pre-linac the energy variation over the bunch train due to multi-bunch beam loading is about 0.15% [3]. Tolerance on the phase at the exit of the second compressor is $|\Delta z| < 10$ μm to limit the relative energy change at the end of the main linac to 0.1%.

The design of the two compressor stages is decribed in Section II. Section III is devoted to residual longitudinal aberrations and their compensation. Section IV discusses the final beam distribution expected from simulations; Section V discusses the spin rotator system. Tuning elements are described in Section VI.

II. COMPRESSOR STAGES

The first stage (BC1), at 2 GeV, consisting of an rf and a wiggler section, rotates the beam by 90 degrees in the longitudinal phase space, to convert initial phase errors due to beam loading in the damping ring into energy errors, and reduces the bunch length by roughly a factor of 10, from about 4 mm to 500 μm. This compression is realized by an rf section that generates a δ-z correlation, followed by a bending section with energy-dependent path length. In this case the bending section is a wiggler consisting of four 90° cells with quadrupoles at zero dispersion points [2]. For a given rf frequency (here L-band), all other parameters are determined by the incoming beam. If the initial energy spread is $\delta \approx 10^{-3}$ the desired bunch length is obtained with $R_{56} = 0.5$ m. Parameters are listed in Table II. In the table, the terms y_a and y_q denote the alignment tolerances for accelerating structures and quadrupoles due to a 1% emittance dilution from single-bunch wakefields or

dispersion, respectively, and the superscript c refers to a compensating rf system discussed in the next section.

After BC1, a 500-m long S-band pre-linac accelerates the beam to 10 GeV. The vacuum pressure in the pre-linac has to be better than 10^{-8} torr. This pressure reduces the emittance dilution expected from filamentation and nonlinear coupling due to ions [4] and alleviates the effect of a predicted fast transverse beam-ion instability [5]. After the pre-linac, the second compressor stage (BC2) at 10 GeV performs a 360-degree rotation in phase space, and reduces the bunch length to 100 μm, appropriate for injection into the main X-band linac. A 360- (or 180-) degree rotation is required to prevent bunch-to-bunch energy errors caused by beam loading in the pre-linac, or phase errors in the damping ring, from translating back into phase errors in the main linac. An arc, a second rf section, and a chicane are the components of BC2. Two parameters may be selected independently, for instance the rf frequency and the R_{56} of the chicane. For the S-band rf chosen, the waveform is more linear and transverse wakefields are less severe than for X-band. The additional length required is a disadvantage of S-band frequency. To reduce the nonlinearities in the longitudinal transformation (T_{566} term in TRANSPORT notation [6]) the R_{56} of the chicane is rather small, namely 36 mm. The necessary rf voltage V_{rf} is then 3.87 GV and the length of the accelerating section is large: 200 m. The arc comprises 60 FODO cells of separated function magnets and does not include distributed sextupoles, the alignment tolerances for which would be severe; its R_{56} can be easily adjusted with the horizontal phase advance. The chicane is constructed from four 10-m bending sections [2]. More parameters are given in Table II. Where two values are listed in the table, the first refers to the arc, the second to the chicane. Note that the horizontal emittance increases by about 2.6% due to synchrotron radiation in wiggler, arc and chicane.

A single-stage compressor does not appear to be a viable alternative to the two-stage design, because the final energy spread of 5% would increase both the effect of nonlinearities in the longitudinal phase space (see next section) and the sensitivity to incoming phase variations. This energy spread would furthermore make transverse emittance preservation a difficult task.

Table 2. Parameters for the two compressor stages.

	1. stage	2. stage
Energy	2 GeV	10 GeV
σ_z	4 mm $\rightarrow$ 500 μ	500 $\mu \rightarrow$ 100 μ
σ_e	0.1% $\rightarrow$ 1.0%	0.25% $\rightarrow$ 2.1%
V_{rf}	136 MV	3.87 GV
f_{rf}	1.4 GHz	2.8 GHz
L_{rf}	9 m	200 m
R_{56}	0.5 m	-0.217 m, 36 mm
'R_{56}' length	100 m	370 m, 210 m
$\Delta\epsilon_{x,SR}/\epsilon_x$	1.3%	1.3%, 0.05%
bend hor. aperture	3 cm	10 cm
y_a	40 μ	~ 8 μ
y_q	17 μ	~ 8 μ
V^c_{rf}	6.9 MV	276 MV
f^c_{rf}	2.8 GHz	11.4 GHz
L^c_{rf}	0.5 m	8 m
total length	110 m	800 m

III. LONGITUDINAL ABERRATIONS

Second-order dependence on energy of the path-length (i.e., T_{566} transfer-matrix element) in wiggler and chicane introduces an important nonlinear aberration in the longitudinal phase space [7]. This nonlinearity causes a strong sensitivity of the final energy at the end of the main linac to the initial phase. The T_{566} is proportional to the R_{56}: for wiggler and chicane $T^{w,c}_{566} = -\frac{3}{2}R^{w,c}_{56}$ and for the arc $T^a_{566} \approx 1.9 \cdot R^a_{56}$. The T_{566} transfer-matrix element is harmful for two reasons. First, initial phase errors are converted into energy errors by BC1, which in turn, due to the T^w_{566} of the wiggler, cause a phase offset in the pre-linac. The result is an additional energy change that may either add to or cancel the previous energy error, depending on the sign of the offset. The energy error is further enhanced by BC2 and, due to the T^c_{566} of the chicane, a significant phase error in the main linac is generated. A second effect is that, depending on the sign of the phase error, the T_{566} can either increase or counteract the nonlinearity of the rf over the bunch, giving rise to an asymmetry of bunch length versus phase error, for each compressor stage separately. To reduce these harmful effects, a small value of 36 mm was chosen for the R_{56} of the chicane.

Even then the residual nonlinear effects are still so large that they need to be compensated. In the proposed design this is done by an additional, decelerating rf system in each compressor stage. The required compensating rf voltage is

$$V^c_{rf} = -2\frac{T^{w,c}_{566}}{R^{w,c}_{56}}\frac{f^2_{rf}eV^2}{{f^c_{rf}}^2E} = 3\frac{f^2_{rf}eV^2_{rf}}{{f^c_{rf}}^2E}, \qquad (1)$$

where E is the beam energy, e the electron charge, and the superscripts w and c refer to wiggler or chicane. The voltage V^c_{rf} is about 7 MV and 300 MV for an S-band and an X-band compensation in BC1 and BC2, respectively.

The residual longitudinal aberrations are now of third order and higher. An initial phase error or multi-bunch beam loading may cause an energy offset δ of the entire bunch at the entrance to BC2. In addition, the longitudinal wakefields in the pre-linac induce a mainly quadratic correlation between energy and the longitudinal position z of a single particle with respect to the bunch center. Due to the R^a_{56} of the arc, the total energy error translates into a position error at the two rf systems of BC2, which is transformed once more into energy by the rf, and back into longitudinal phase by the T^c_{566} of the chicane. The final phase z_f of a single particle at the exit of BC2 is

$$z_f \approx az - bz^4 - c\delta^2z^2 - d\delta z^2 - e\delta z^4 + \ldots \qquad (2)$$

where $a \approx 1/5$–$1/7$ is the desired linear compression ratio, and the four nonlinear terms on the right-hand side are about the same size (10–20 μ), for typical values $\delta \approx \pm 0.004$ and $z \approx 500$ μ. These four terms are negligible if either the T^c_{566} or the pre-linac wakefields are absent.

IV. PERFORMANCE

Computer simulations of the longitudinal single-bunch dynamics are performed with the code LITRACK [8], taking into account the nonlinear rf waveform, T_{566} matrix-

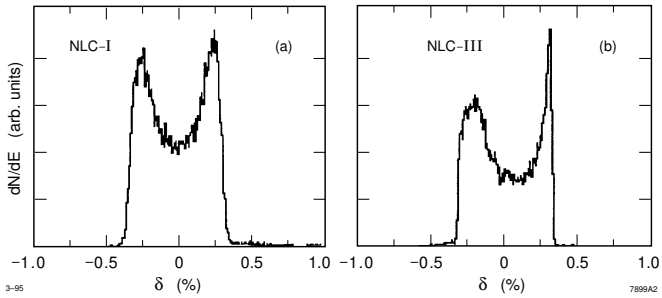

Figure. 2. Energy profile at the end of the main linac for NLC I and NLC III (Table I), and no initial phase error.

elements, and single-bunch longitudinal wakefields. A distribution of particles as extracted from the damping ring is tracked through the different compressor subsystems and the main X-band linac. The full-width-half-maximum energy spread for zero-phase error was chosen to be roughly 0.6%. The simulations show that even for NLC III the final average energy and the rms energy spread at the end of the main linac vary by less than 0.1% for initial phase errors up to 20° S-band. Figure 2 illustrates the energy profile at the end of the main linac for no initial phase error. A deformation of the distribution for NLC-III, due to the increased wakefields in the pre-linac, is clearly evident.

V. SPIN ROTATOR

The spin-rotator system located between the damping ring and BC1 (see Fig. 1), is constructed from two solenoid pairs separated by a 19.83° mini-arc [9]. The two solenoids of each pair are separated by a reflector beamline, whose horizontal and vertical transfer matrices are $+I$ and $-I$, respectively. This cancels the x-y coupling independent of solenoid settings. Each solenoid pair is capable of providing a 90° spin rotation about the longitudinal axis, while the mini-arc rotates the spin by 90° around the vertical axis. In this way arbitrary control over the spin orientation is provided. Relative depolarization in the compressor arc at 10 GeV is less than 1.6%, and total R_{56} of the rotator arc is −40 mm, with no effect on the bunch length after BC1. The chromatic emittance dilution at 0.1% rms energy spread is ∼0.5%.

VI. TUNING AND DIAGNOSTICS

Extensive simulations of tuning and correction schemes have been performed for the spin rotator and for BC1. So far little work has been done for BC2. Corrections in BC2 are not expected to be difficult.

The large energy spread after BC1 sets tight tolerances on the residual dispersion, e.g., the maximum tolerable dispersion for a 2% emittance dilution is about 175 μ behind BC1. Therefore, two orthogonal $-I$ pairs of quadrupoles and skew quadrupoles are placed at large dispersion points in the wiggler section of BC1 for dispersion correction. Two more skew quadrupoles, separated by a phase advance of 90°, are located in the mini-arc section of the spin rotator. These quadrupoles cancel dispersion generated in front of the BC1 rf section. Cross-plane coupling generated in the damping ring or due to imperfections in the rotator system is compensated by a skew correction section (SCS). The SCS follows the spin rotator and contains 4 orthonormal skew quadrupoles (orthogonal and equally scaled) that allow complete decoupling. Four variable quadrupoles match the beam extracted from the damping ring to the rotator optics. To maintain the periodic beta functions in the spin rotator itself for varying solenoid fields, two four-quadrupole beta-matching sections are located in front of and behind the mini-arc. In addition several matching quadrupoles are found between SCS and BC1 and following BC1. The rf in BC1 may be turned off to ease beta matching and decoupling. A correction of second-order dispersion is necessary only if the vertical emittance dilution due to first order dispersion mismatch is larger than a factor of ten. In that case four paired skew sextupoles are added to the wiggler section. Four wire scanners at 45° phase advance intervals are located behind the wiggler and used to adjust the above correctors by minimizing the projected emittance. In addition wire scanners placed at high dispersion points in mini-arc and wiggler measure the extracted energy spread and bunch length, respectively. Tuning simulations with the SLC flight simulator [10] for an initial emittance dilution by a factor 200, due to rms quadrupole field errors of 1% and rms dipole roll errors of 0.25°, result in a final emittance dilution of less than 2%. This tuning procedure would require about 16 hours of real machine time.

VII. CONCLUSIONS

A design of a two-stage bunch compressor for the NLC has been described that meets all specifications, as far as single-bunch dynamics is concerned. A single-stage compressor does not appear to be a viable alternative. Multi-bunch effects in the compressor have not yet been studied in detail. Also the optimimum bunch shape at the exit of BC2 still needs to be determined. A larger value for the $R_{56}^{a,c}$ matrix elements of arc and chicane is desirable, since it would allow a length reduction of the rf section in BC2. It is not yet known if the increased sensitivity to initial phase errors and to energy-errors in the S-band pre-linac would be tolerable.

References

[1] T. Raubenheimer et al., "Parameters of the SLAC Next Linear Collider," these proceedings.
[2] T. Raubenheimer, P. Emma, S. Kheifets, *Proc. of 1993 IEEE PAC*, Washington (1993) 635; T. Raubenheimer, NLC Note 2 (1994).
[3] R. Miller, private communication (1994).
[4] T. Raubenheimer, P. Chen, SLAC-PUB-5893 (1992).
[5] T. O. Raubenheimer and F. Zimmermann, SLAC-PUB-6740 (1995).
[6] K. Brown, F. Rothacker, D. Carey, C. Iselin, SLAC-91 (1977).
[7] F. Zimmermann, NLC Note 3 (1994).
[8] The program LITRACK was written by K. Bane.
[9] P. Emma, NLC Note 7 (1994).
[10] M. Woodley, private communication (1994).